Energy Conversion and Management 52 (2011) 1638–1643

Contents lists available at ScienceDirect

Energy Conversion and Management

journal homepage: www.elsevier.com/locate/enconman

A numerical investigation of the geometric effects on the performance of plate finned-tube heat exchanger

Chi-Wen Lu [a], Jeng-Min Huang [a], W.C. Nien [a], Chi-Chuan Wang [b,*]

[a] Department of Refrigeration, Air Conditioning and Energy Engineering, National Chin-Yi University of Technology, No. 35, Lane 215, Chung-Shan Rd., Sec. 1, Taiping City, Taichung County 411, Taiwan
[b] Department of Mechanical Engineering, National Chiao Tung University, 1001 University Road, 300 Hsinchu, Taiwan

ARTICLE INFO

Article history:
Received 10 June 2009
Received in revised form 8 February 2010
Accepted 15 October 2010
Available online 20 November 2010

Keywords:
Fin-and-tube heat exchanger
Axial fan
CFD

ABSTRACT

This study numerically examines the geometric parameters on the performance of a two-row fin-and-tube heat exchanger. Effects of fin pitch, tube pitch, fin thickness, and tube diameter are termed with. The simulation indicates that the performance, in terms of $Q/\Delta P$ and COP, increases with longitudinal tube pitch or with transverse tube pitch, and it decreases with larger tube diameter or fin thickness. An optimum value for $Q/\Delta P$ occurs at a 6–8 fpi at a fixed flow rate condition. There is not much difference in choosing the index of $Q/\Delta P$ or COP under fixed flow rate condition. However, when the simulation are performed with the actual axial fan whose P–Q curve being implemented. It is found that $Q/\Delta P$ peaks at 12 fpi while COP peaks at 16 fpi.

1. Introduction

Finned-tube heat exchangers are frequently used in HVAC&R applications. Its easier manufacturing, simpler construction, lower cost, and relatively easy in maintenance make it one of the most commonly used heat exchangers. The performance of fin-and-tube heat exchangers are related to many geometric parameters such as fin pitch, tube pitch, tube size, and fin thickness. It is quite difficult to achieve the best performance subject to these parameters in the early days. This is because results normally relied on experimentation and it is very unlikely to examine all kind of geometric influences from the manufacturing fin-and-tube heat exchangers. Hence, early experimental studies conducted by Rich [1,2], who investigated a total of fourteen coils, in which the tube size were 13.34 mm. The corresponding longitudinal and transverse tube pitches were 27.5 and 31.75 mm, respectively. He examined the effect of fin spacing and the number of tube row, and concluded that the heat transfer coefficient was essentially independent of the fin spacings and the pressure drops per row is independent of the number of tube rows.

McQuiston [3] provided test results for five heat exchangers ([3], Fp = 1.81–6.35 mm, D_o = 9.96 mm, P_l = 22 mm, P_t = 25.4 mm, and Row = 4), and he later [4] proposed the first popular correlation by employed a “finning factor”, defined as A_o/A_{to}, to correlate his data along with those by Rich [1,2]. A strong dependence of heat transfer performance with the finning factor was observed. McQuiston [4] showed an $(A_o/A_{to})^{-0.15}$ dependence in his correlation. The friction factor correlation proposed by McQuiston [4] claimed to have ±35% accuracy. Based on the previously published data, Gray and Webb [5] developed a correlation to correlate the existing experimental data. The root-mean-square error of the resulting correlation was 7.3% for heat transfer coefficients, and 7.8% for friction factors. Seshimo and Fujii [6] had provided test results for a total of 35 samples. Unfortunately, their test range was limited to 0.5 m s^{-1} < V_{fr} < 2.5 m s^{-1}. Wang et al. [7] had presented fifteen samples of plain fin-and-tube heat exchangers to examine the effect of several geometrical parameters, including the number of tube rows, fin spacing, and fin thickness but their test samples were limited to one configuration. Rosman et al. [8] conducted heat transfer experiments on a two-row exchanger, and compared his test results with some previous studies with good accuracy. However, the foregoing results were limited to certain configuration and results were based on the tested samples.

A more comprehensive experimental study concerning parametric influences and its correlation on the air side performance having plain fin configuration had been carried out by Wang and Chi [9] and Wang et al. [10]. Some influences such as the number of tube row, fin pitch and tube size on the air side performance had been reported. Madi et al. [11] also examined the relevant geometric influences (fin pitch, fin thickness and tube pitch) for 28 samples, including 7 plain fins and 21 wavy fins. Their test results indicated smaller fin thickness result in higher heat transfer

* Corresponding author.
E-mail address: ccwang@mail.nctu.edu.tw (C.-C. Wang).

0196-8904/$ - see front matter © 2010 Elsevier Ltd. All rights reserved.
doi:10.1016/j.enconman.2010.10.026

Nomenclature

A_o	total surface area, m^2	N	the number of tube row
A_{to}	outside surface area of tube	P_l	longitudinal tube pitch, mm
C_p	specific heat of constant pressure, J kg^{-1} K^{-1}	P_t	transverse tube pitch, mm
COP	performance index, COP = $Q/(\Delta P \cdot \dot{V})$, coefficient of performance	Pr	Prandtl number
d_c	fin collar outside diameter, mm	ΔP	pressure drop, Pa
D_h	hydraulic diameter, m	Q	heat transfer rate, W
F_p	fin pitch, mm	Re_{D_h}	Reynolds number based on hydraulic diameter
h	heat transfer coefficient, W m^{-2} K^{-1}	V_{fr}	frontal velocity, m s^{-1}
L	depth of the heat exchanger, m	$\dot{V}$	volume flow rate, m^3 s^{-1}
		x^+	reciprocal of the inverse Graetz number

coefficient. Wongwises and Chokeman [12] investigated the effects of a fin pitch and number of tube rows on the air side performance of fin-and-tube heat exchangers having herringbone wavy fin configuration at various fin thicknesses. The experimental results revealed that the fin pitch has an insignificant effect on the heat transfer characteristic. The friction factor increases with increasing fin pitch when $Re_{Dc} > 2500$. Ma et al. [13] studied the air side heat transfer and friction characteristics of wavy fin-and-tube heat exchangers with and without hydrophilic coating, their results indicated that the influence of the hydrophilic coating on heat transfer performance is mainly related to the flow conditions of condensation water on the fin surface without hydrophilic coating. The aforementioned study was mainly based on experimental test results. Despite numerous experimental data were reported, the optimum performance of the associated heat exchangers are still unavailable due to limitation of practical manufacturing. With the advent of high performance computational power, researchers like Fiebig et al. [14] or Jang et al. [15] exploitation of numerical tools to study the complex interactions amid geometric parameters of fin-and-tube heat exchangers are therefore feasible. Hence it is the objective of this study to examine the optimization of fin-and-tube heat exchangers through numerical calculations. The simulations are first conducted at a fixed flow rate to examine the best performance and then further calculations are performed with practical fan/exchanger combinations.

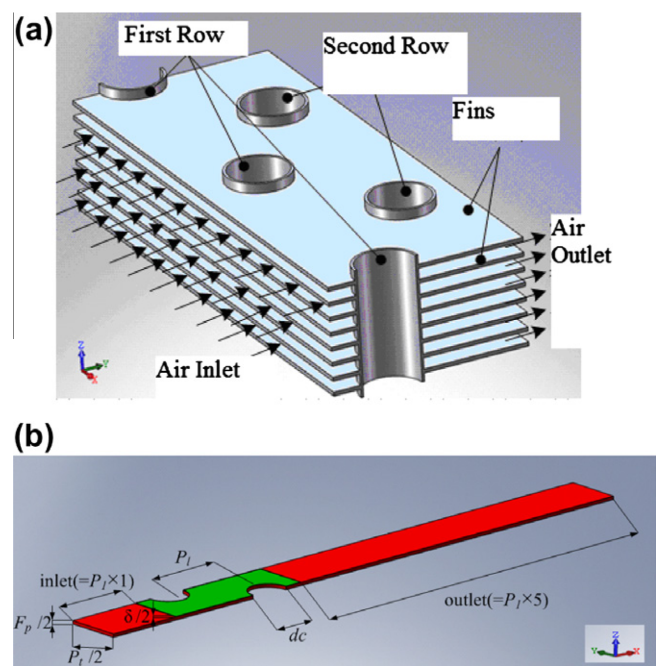

Fig. 1. Schematic of the computational domain for (a) the heat exchanger; (b) actual computational domain (including prior and posterior extension).

2. Physical model, governing equations and numerical method

In this study, simulations are made with staggered fin-and-tube heat exchangers having plain fin configuration. Influences of frontal velocity, tube pitch, tube size, and fin thickness on the air side performance are examined in this study. A schematic of the heat exchanger is depicted in Fig. 1a while the associated computational domain is shown in Fig. 1b. Some detailed geometric parameters for conducting the simulations are tabulated in Table 1 and the physical properties of air and aluminum are tabulated in Table 2. As the airflow flows across the fin-and-tube heat exchanger is actually a quite complex one involving complex interactions amid flow field and obstacles (tube and fins). Hence some assumptions are made in the following to simplify the calculation:

Table 1
Geometric details of the simulated heat exchanger (unit: mm).

Depth	Additional extension section at the entrance	Additional extension section at the outlet	F_p	P_t	P_l	V_{fr}	d_c	δ_f
			6.350					
				20.0		1.2		
			4.235		15		6	0.080
				25.4		1.4		
			3.175		19.05		8	0.115
38.1	19.05	95.25		30.0		1.6		
			2.115		23		10	0.160
				35.0		1.8		
			1.590		27		12	0.200
				40.0		2.0		
			1.265					

(1) Steady state prevails.
(2) Buoyancy force is neglected.
(3) The heat transfer is via sensible heat only, no mass transfer is being taken place.
(4) Incompressible flow, constant properties.
(5) Effects of heat dissipation and thermal radiation are negligible.
(6) Smooth surface conditions for the fin-and-tube.

The corresponding boundary conditions used for simulations are:

(1) No slip conditions at the solid surfaces.
(2) Conjugate heat transfer prevails amid fin and airflow.

Table 2
Properties of the fin material and air.

	Density ($kg\ m^{-3}$)	Specific heat ($J\ kg^{-1}\ k^{-1}$)	Thermal conductivity ($W\ m^{-1}\ K^{-1}$)	Dynamic viscosity ($kg\ m^{-1}\ s^{-1}$)
Fin	2702	903	237	
Air	1.205	1006	0.02637	1.81×10^{-5}

(3) The tube wall temperature is fixed at 328 K. This is typically applicable for a condenser situation.
(4) Additional extension sections prior to and posterior to the heat exchanger are included in the simulation, and their corresponding length are given in Table 1. The uniform velocity assumption is given at the entrance of the extension section. A free-gradient outlet boundary condition is set at the exit of downstream extension.
(5) The "symmetry" boundary is set at the two symmetrical planes.

A commercial CFD code Star-CD is used in this study to calculate the flow and temperature fields of the fin-and-tube heat exchangers. Except Leu et al. [16] using standard K–ε turbulent model, most previous researches like Jang et al. [15] and Mendez et al. [17] used laminar flow equations in the simulation of fin-and-tube heat exchanger. In this study, the wake flow at the exit of heat exchanger might be in transition or in turbulent flow region. Therefore simulation may not converge by the laminar flow model. In this regard, low-Reynolds number K–ε model is applied in this study in order to calculate a mixed flow fields (combined laminar, transition and turbulent flow types) as suggested by Huang et al. [18]. A test of low-Reynolds model is performed to examine the applicability of this model in the mixed flow field. Firstly, low-Reynolds model is used to calculate a fully laminar flow field (a heat exchanger with 0.2 $m\ s^{-1}$ inlet air velocity). The solution is almost the same as that of calculation from the laminar equations. The eddy viscosities are very small compared with molecular viscosities. This indicates that the low-Reynolds number turbulent model can be directly applied even at the laminar flow region. Then the inlet air velocity is increased to 2 $m\ s^{-1}$, calculated results of the flow field shows that the eddy viscosities of the flow between fins are near zero, suggesting a laminar flow region prevails. However, the eddy viscosity increases rapidly as the flow leaving the fins. In fact, the highest eddy viscosity in the wake is about 70 times higher than molecular viscosity ($1.5 \times 10^{-5} m^2\ s^{-1}$). Hence the flow is no longer laminar.

The following equations are used in this study:

- Low-Reynolds number K–ε turbulence model momentum equation (air side).
- Low-Reynolds number K–ε turbulence model energy equation (air side).
- Heat conduction equation (fins).

Detailed description of the turbulent model can be found in the Star-CD user's manuals. The mesh used in the study is shown in Fig. 2. Due to the complexity of fin–tube geometry, an unstructured

Table 3
Results of grid dependence check.

Cell	Heat transfer rate (W)	Relative error (%)
39,200	0.4381609	
		0.6113
106,500	0.4354986	
		0.3078
203,400	0.4341621	

Sample heat exchanger with P_t = 25.4 mm, P_l = 19.05 mm, d_c = 10 mm, F_p = 1.59 mm, δ_f = 0.115 mm, V_{fr} = 1.6 $m\ s^{-1}$.

Table 4
Comparison between experimental heat transfer coefficients (h, $W\ m^{-2}\ K^{-1}$) [8] and the present simulation.

V_{fr} ($m\ s^{-1}$)	Computational results	Experimental results [8]	Deviation (%)
1.20	51.44	47	8.64
1.34	53.17	50	5.96
2.35	64.26	63.5	1.19
6.20	100.68	101	0.31

Heat exchanger dimensions: P_t = 25.4 mm, P_l = 19.05 mm, d_c = 10.23 mm.

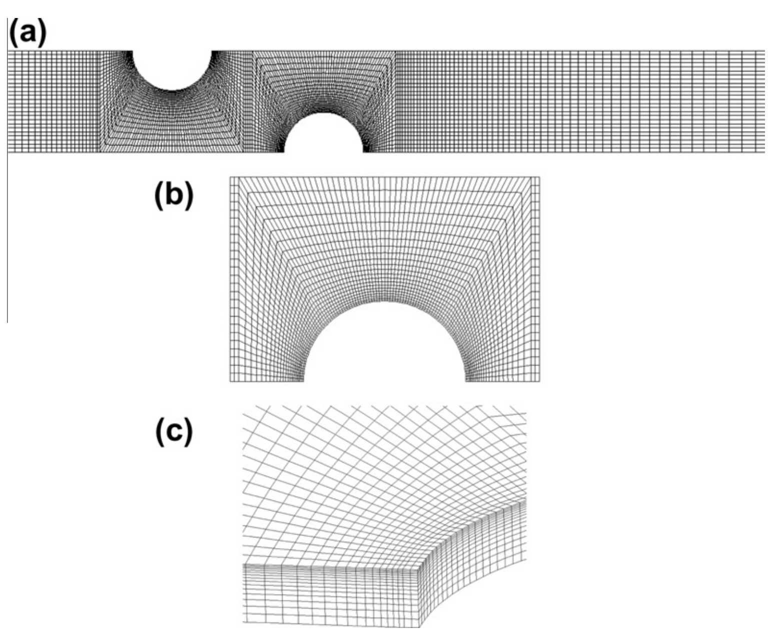

Fig. 2. Schematic of the computational grid structure (a) for the whole heat exchanger; (b) adjacent to the round tube; and (c) nearby the fin.

grid system is generated by "Auto Mesh" function of Star-CD for the airflow channel and the structured grid is used in the solid part. Star-CD is a finite-volume based CFD package. The central difference method is used to discretize the diffusion term and the convection term is discretized by upwind difference method. Simple scheme is applied on the iteration procedure. Numerical convergence is accepted only when the residuals of velocities, pressure, temperature and turbulent kinetic energy are smaller than 10^{-5}.

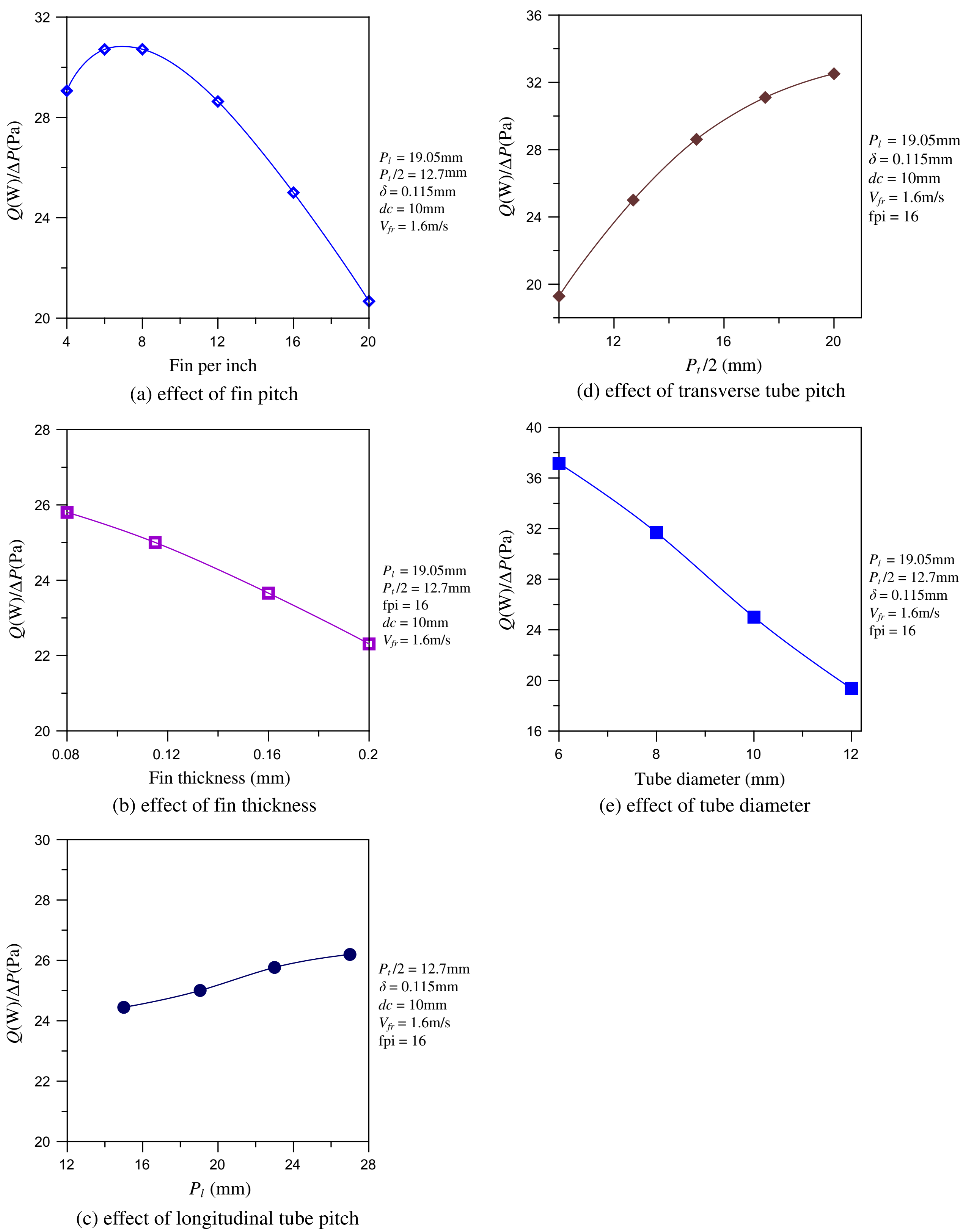

Fig. 3. Influence of geometric parameters for (a) fin pitch; (b) fin thickness; (c) longitudinal tube pitch; (d) transverse tube pitch and (e) tube diameter on the performance index $Q/\Delta P$ at a fixed frontal velocity of 1.6 m s^{-1}.

Grid dependence check is carried out and results are tabulated in Table 3. Typical grid sizes are from 106,500 and 203,400. To avoid the run-off error resulting from numerical instability, double precision is used throughout the computation.

3. Results and discussion

In order to validate the accuracy of the simulation, calculations are compared with the experimental work from Wang and Chi [9], and the comparisons are tabulated in Table 4. As seen in the table, the deviation between numerical and experimental results is less than 10%, which is within the typical experimental uncertainty (3%–15%). From the above validation, it is concluded that the simulation software is capable of solving the heat exchanger problem with reasonable accuracy.

The following calculations are then carried out for a two-row fin-and-tube heat exchanger with its characteristic dimension being 145 mm $(W) \times 127$ mm $(H) \times 38.1$ mm (L). The effects of fin number, fin thickness, transverse tube pitch, and longitudinal tube pitch on overall performance of the heat exchanger is then investigated. For a better characterization of the relevant effects, the performance of heat exchanger is termed $Q/\Delta P$ and $Q/(\Delta P \cdot \dot{V})$ as the evaluation index. Where Q is the heat exchange rate, ΔP is the pressure drop across the heat exchanger, and $\dot{V}$ is the volumetric flow rate. In the subsequent discussion, $Q/(\Delta P \cdot \dot{V})$ is designated as COP for it represents the ratio amid actual heat transfer rate and the provided pumping work.

The effect of individual parameters, such as fin pitch, fin thickness, longitudinal tube pitch, and transverse tube pitch on overall performance is respectively depicted in Fig. 3. Most of the geometric parametric influence, except fin pitch, shows an asymptotic trend. For instance, $Q/\Delta P$ dwindles with the rise of tube diameter and of fin thickness. In the meantime, $Q/\Delta P$ steadily increases with the rise of longitudinal tube pitch and of transverse tube pitch. These results are expected the associated reduction of pressure drops outperforms heat transfer rate in the former and is opposite in the latter. However, an unusual optimal phenomenon is encountered concerning the influence of fin pitch. It is interesting to know that $Q/\Delta P$ peaks at a fin pitch around 6–8 fpi. Apparently one can expect a rise of heat transfer rate and pressure drop by adding surfaces. In general the pressure drop outlasts heat transfer and exhibits a decreasing trend of $Q/\Delta P$ when the fin pitch is reduced. The heat transfer performance of a fin-and-tube heat exchanger is actually associated with the interactions of airflow with tubes and fins. For a plain channel without tube interruption, its performance is strongly related to simultaneous developments of flow and temperature field, yet the influence of the entrance development is related to the reciprocal of the inverse Graetz number x^+, which is defined as

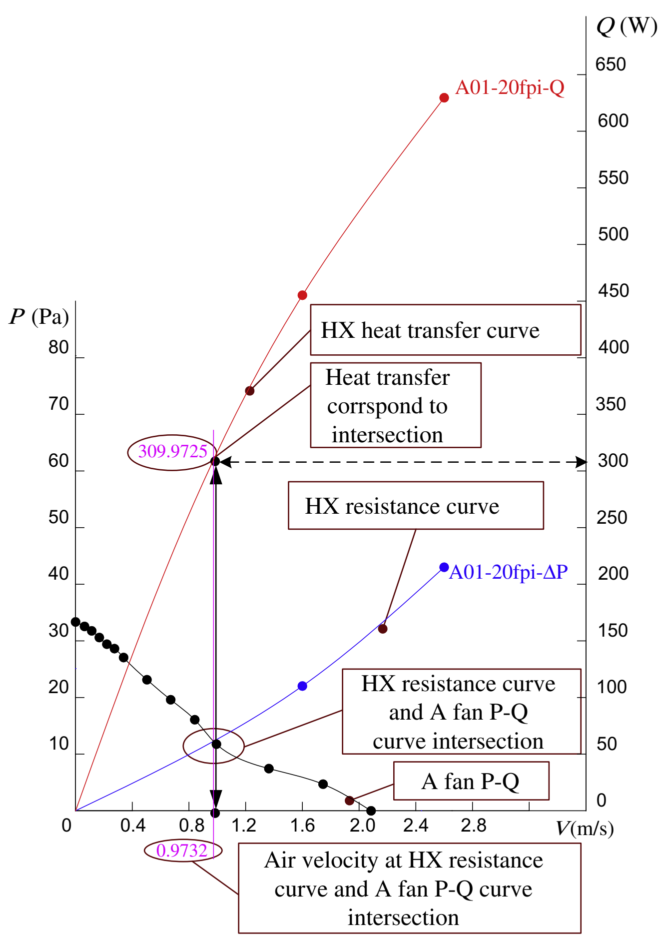

Fig. 4. Actual performance subject to the flow resistance and P–Q fan curve of a axial fan.

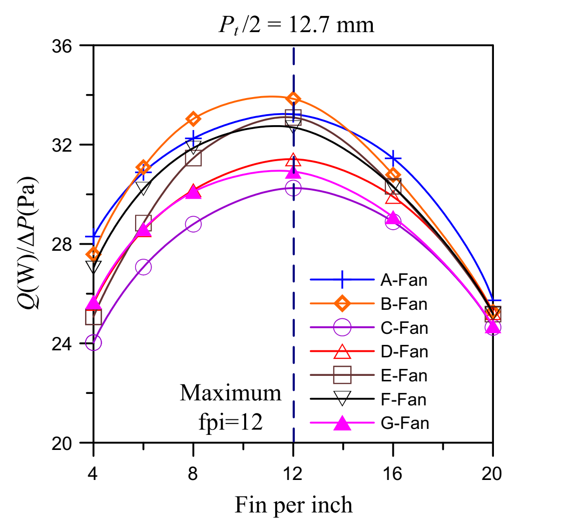

Fig. 5. Influence of fin pitch subject to actual fan curve on the performance index $Q/\Delta P$ at a fixed frontal velocity of 1.6 m s^{-1}.

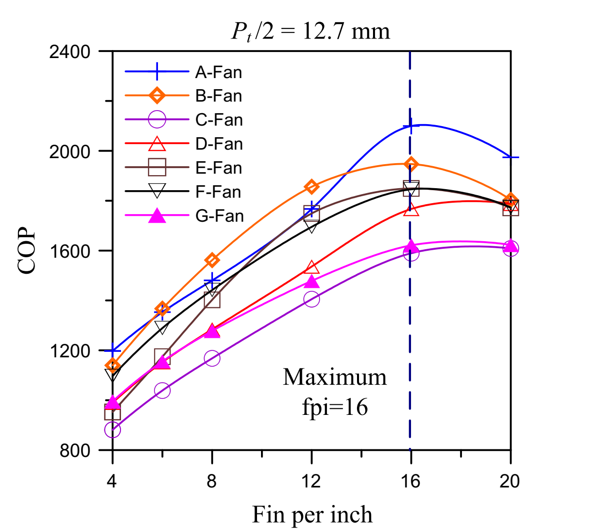

Fig. 6. Influence of fin pitch subject to actual fan curve on the performance index COP at a fixed frontal velocity of 1.6 m s^{-1}.

$$x^{+} = \frac{L/D_h}{Re_{D_h}\mathrm{Pr}} \tag{1}$$

where L is the streamwise duct length and Pr is the Prandtl number. The flow may be considered to be fully developed when $x^{+} > 0.04$ [19]. The developing length for a very low fin pitch such as 20 fpi is only as low as 3–4 mm, indicating the major portion of fin-and-tube heat exchangers fall into the fully developed category thereby giving rise to a lower performance as the fin pitch is reduced. In the meantime, the presence of tube row provides an augmentation to heat transfer by generating longitudinal vortices and unstable defected swing flow (Coanda effect). These two augmented effects are more conspicuous when fewer fin surfaces is present and an opposed influence is imposed on these two heat transfer augmentation mechanisms when fin surface is increased. This is because adding fin surface inevitably stabilizes the flow field and lessens the contributions of vortices and unstable flow field. As a consequence, one can see a maximum value of $Q/\Delta P$ occurring adjacent to a fin pitch of 6–8 fpi. Notice that other geometric effects such as fin thickness, longitudinal tube pitch, and transverse tube pitch do not processes such unusual characteristic.

The foregoing results are conducted at a fixed flow rate (frontal velocity). Normally heat exchangers are accompanied with fans to fulfill the heat transfer duty. The actual performance of the heat exchangers depends on the interactions amid fan and heat exchangers. Therefore, the present study had investigated the associated influences of fans on the overall performances. This is made by selecting some commercially available axial fans whose performances are available in terms of P–Q curves. Implementing the actual P–Q curves subject to the simulated pressure drop of the heat exchanger, one can therefore obtain the actual flow rate and its heat transfer rate at a specific fin pitch. As a result, we can obtain a similar $Q/\Delta P$ vs. fpi subject to actual fan performance as shown in Fig. 5. Analogously, the graph of $Q/\Delta P$ vs. fin pitch also exhibits a bulge phenomenon, yet the maximum value is quite independent of fans occurring at a fin pitch of 12 fpi as compared to 6–8 fpi at a fixed flow rate. The shift of the optimum fin pitch toward to a higher value is actually in connected with the fan P–Q curve itself. As can be seen from a typical P–Q curve of an axial fan in Fig. 4, moderate or large flow rate are encountered at a lower pressure drop region while significant static pressure rise occurs only when the flow rate is less than half of the maximum flow rate. This phenomenon is in conjunction with the characteristics of axial flow fan and is applicable to all the axial fans tested in this study. As a result, despite lower flow resistance occurs at a low flow rate for a very low fin pitch, the amount of surface area could not fulfill a larger heat duty, leading to a lower $Q/\Delta P$. In the meantime, surplus surface area not only provides a higher flow resistance but also decrease the heat transfer performance (as aforementioned in foregoing section), hence considerable decline of $Q/\Delta P$ is seen for larger fin pitch. Summation of these two extremes and the maximum occurs at a fin pitch of 12 fpi which is much higher than simulation at a fixed flow rate. Interestingly, the locus of all the tested fans is quite similar and they all peak at 12 fpi. This is again due to the similar P–Q curve of the axial fans. Correspondingly, COP vs. fpi also reveals similar trend but its peak value had been shifted to about 16 fpi, as shown in Fig. 6. Notice that the disparity between COP and $Q/\Delta P$ comes from the effect of flow rate. Yet a larger fin surface limits the airflow rate, thus a higher value of COP moves toward a larger fin pitch.

4. Conclusion

This study numerically examines the geometric parameters on the air side performance of a two-row fin-and-tube heat exchanger. Effects of fin pitch, tube pitch, fin thickness, and tube diameter on the performance of heat exchanger is investigated. The performance is termed with are termed with $Q/\Delta P$ and COP. Major conclusions from the simulations are given as follows:

(1) The performance of fin-and-tube heat exchanger, $Q/\Delta P$, dwindles with the rise of tube diameter and of fin thickness. In the meantime, $Q/\Delta P$ steadily increases with the rise of longitudinal tube pitch and of transverse tube pitch.
(2) A optimum value for $Q/\Delta P$ vs. fin pitch is encountered and it occurs at a 6–8 fpi at a fixed flow rate condition. This is because higher fin pitch may result in fully developed flow and deteriorate the overall performance, yet a substantial rise of heat transfer caused by vortex and unstable is observed when fin surfaces are considerably removed.
(3) There is not much difference in choosing the index of $Q/\Delta P$ or COP under fixed flow rate condition. However, when the simulation are performed with the actual axial fan whose P–Q curve being implemented. It is found that $Q/\Delta P$ peaks at 12 fpi while COP peaks at 16 fpi.

Acknowledgement

The authors would like to thank some financial support from the National Science Council (99-2218-E-009-012-MY2) of Taiwan.

References

[1] Rich DG. The effect of fin spacing on the heat transfer and friction performance of multi-row, smooth plate fin-and-tube heat exchangers. ASHRAE Trans 1973;79(1):137–45.
[2] Rich DG. The effect of the number of tube rows on heat transfer performance of smooth plate fin-and-tube heat exchangers. ASHRAE Trans 1975;81(1):307–17.
[3] McQuiston FC. Heat, mass, and momentum transfer data for five plate-fin-tube heat transfer surfaces. ASHRAE Trans 1978;84(1):266–93.
[4] McQuiston FC. Correlation of heat, mass, and momentum transport coefficients for plate-fin-tube heat transfer surfaces with staggered tubes. ASHRAE Trans 1978;109(1):294–308.
[5] Gray DL, Webb RL. Heat transfer and friction correlations for plate finned-tube h e at exchangers having plain fins. In: Proceedings of eighth heat transfer conference; 1986. p. 2745–50.
[6] Seshimo Y, Fujii, M. An experimental study of the performance of plate fin and tube heat exchangers at low reynolds number, In: Proceeding of the third ASME/JSME thermal engineering joint conference, vol. 4; 1991. p. 449–54.
[7] Wang CC, Hsieh YC, Chang YJ, Lin YT. Sensible heat and friction characteristics of plate fin-and-tube heat exchangers having plane fins. Int J Refrig 1996;19:223–30.
[8] Rosman EC, Carajilescov P, Saboya FEM. Performance of one and two-row tube and plate fin heat exchanger. J Heat Transfer 1984;106:627–32.
[9] Wang CC, Chi KU. Heat transfer and friction characteristics of plain fin-and-tube heat exchangers. Part I: New experimental data. Int J Heat Mass Transfer 2000;43:2681–91.
[10] Wang CC, Chi KU, Chang CJ. Heat and friction characteristics of plain fin-and-tube heat exchangers. Part II: Correlation. Int J Heat Mass Transfer 2000;43:2693–700.
[11] Madi AM, Johns RA, Heikal MR. Performance characteristics correlation for round tube and plate finned heat exchangers. Int J Refrig 1998;21:507–17.
[12] Wongwises S, Chokeman Y. Effect of fin pitch and number of tube rows on the air side performance of herringbone wavy fin-and-tube heat exchangers. Energy Convers Manage 2005;46:2216–31.
[13] Ma X, Ding G, Zhang Y, Wang K. Effects of hydrophilic coating on air side heat transfer and friction characteristics of wavy fin-and-tube heat exchangers under dehumidifying conditions. Energy Convers Manage 2007;48:2525–32.
[14] Fiebig A, Grosse-Gorgemann Y, Chen Y, Mitra NK. Conjugate heat transfer of a finned. Part A: Heat transfer behavior and occurrence of heat transfer reversal. Numer Heat Transfer 1995;A28:133–46.
[15] Jang JY, Wu MC, Chang WJ. Numerical and experimental studies of three-dimensional plate-fin-and-tube heat exchangers. Int J Heat Mass Transfer 1996;39:3057–66.
[16] Leu JS, Wu YH, Jang JY. Heat transfer and fluid flow analysis in plate-fin-and-tube heat exchangers with a pair of block shape vortex generators. Int J Heat Mass Transfer 2004;47:4327–38.
[17] Mendez RR, Sen M, Yang KT, Clain RM. Effect of fin spacing on convection in a plate fin-and-tube heat exchanger. Int J Heat Mass Transfer 2000;43:39–51.
[18] Huang JM, Hsieh WC, Ke XJ, Wang CC. The effects of frost thickness on the heat transfer of finned tube heat exchanger subject to the combined influence of fan types. Appl Therm Eng 2008;28:728–37.
[19] Sergent JE, Krum A. Thermal management handbook for electronic assemblies. New York: McGraw-Hill; 1998.